Rheological, Electrokinetic, and Morphological Characterization of Alginate–Bentonite Biocomposites

B. Benli,[1] F. Boylu,[1] M. F. Can,[2] F. Karakaş,[1] K. Çinku,[3] G. Ersever[4]

[1]*Mineral Processing Department, Istanbul Technical University, Ayazaga, Istanbul, Turkey*
[2]*Mining Engineering Department, Engineering Faculty, Afyon Kocatepe University, Afyon, Turkey*
[3]*Mining Engineering Department, Engineering Faculty, University of Istanbul, Istanbul, Turkey*
[4]*Mining Engineering Department, Engineering Faculty, Dumlupınar University, Kütahya, Turkey*

Received 25 March 2010; accepted 8 October 2010
DOI 10.1002/app.33627
Published online 18 April 2011 in Wiley Online Library (wileyonlinelibrary.com).

ABSTRACT: We prepared biocomposite gel dispersions involving sodium alginate (Na-Alg) and calcium bentonite (Ca-B) with various solid concentrations and characterized their rheological, electrokinetic, and morphological properties. The flow properties, such as the apparent and plastic viscosities, shear stress, and yield value point, changed with increasing clay dosage. The viscosities of the homogeneous dispersions were represented by the Herschel–Bulkley model. The ζ-potential results were examined in the light of different characterization methods (X-ray diffraction, Fourier transform infrared spectroscopy, and atomic force microscopy) to understand the interactions between the Na and Ca ions of the alginate biopolymer and bentonite clay. A plausible structural model for the alginate–bentonite composite gel, known as the *egg-box model,* is proposed. The presence of Ca ions in the Ca-B partially crosslinked Na-Alg may be regarded as an excellent example of a self-assembling process. © 2011 Wiley Periodicals, Inc. J Appl Polym Sci 122: 19–28, 2011

Key words: biopolymers; clay; atomic force microscopy (AFM); rheology; ion exchangers

INTRODUCTION

Sodium alginate (Na-Alg), in addition to its well-known features, such as nontoxicity, biocompatibility, biodegradability, hydrophilicity, and relatively low cost,[1–3] has been used extensively because of its unique properties of gel formation—covalent crosslinking with divalent ions, which forms what is known as an *egg-box junction.*[4,5] Therefore, as a biopolymer, it has maintained its diverse utility for more than a decade, especially in biomedical applications, such as wound dressings,[6] tissue engineering scaffolds,[7] drug-delivery carriers,[8] food applications involving coating materials in improved encapsulation,[9] antibacterial alginate-based edible films,[10] and biobased packaging materials in various food categories.[11] Alginate has been of commercial interest in the food industry as an emulsifier, thickener, and stabilizer since its recognition in the 1930s.[12]

Bentonite is commercially known as *montmorillonite* and is a layer-structured clay in the smectite group of minerals.[13] Smectite-group clay minerals have large adsorption capacities for polymer molecules because of their unique crystal structure.[14] The polymers in the montmorillonite dispersions interacted with the clay particles according to their ionic or nonionic character. The ionic polymers induced electrostatic interactions, but the nonionic polymers were adsorbed on the surface of the clay minerals by their steric interactions. The polymer concentration, molecular weight and hydrolyzing groups, size and shape of the clay particles, surface charge, clay concentration in suspension, pH, and temperature may all affect the clay/polymer interactions. The adsorption of polymers onto the surfaces of clay particles influences the rheology and electrokinetic properties of the system. The rheological behavior of the suspensions is one of the most sensitive indicators for the determination of particle interactions, which can drastically change with even small variations in the composition of the medium.[15] Other alternatives include the synthesis of biopolymer/inorganic nanocomposites, which have many advantages over biocomposites. Recently, biodegradable polysaccharide/layered silica clay nanocomposites have been investigated because they exhibit markedly improved mechanical, optical, thermal, and physicochemical properties and decreased gas/vapor permeability, reduced flammability, and controlling release properties compared with pure polysaccharides.[16(a)] Although the effects of polymers[17] and dyes[18,19] on montmorillonite dispersions have been studied extensively, the interaction mechanism between Na ions of alginate and Na/Ca ions of bentonite has not been understood well because of the lack of a systematic investigation.

Correspondence to: F. Boylu (boylu@itu.edu.tr).

© 2011 Wiley Periodicals, Inc.

In this study, the effects of alginate biopolymer on the rheological and electrokinetic properties of calcium bentonite (Ca-B) dispersions at various solid concentrations were investigated. ζ-potential (zp) measurements and morphological characterization by X-ray diffraction (XRD), Fourier transform infrared (FTIR) spectroscopy, and atomic force microscopy (AFM) were conducted to elucidate the adsorption mechanism and rheological response of the dispersions. Possible structural models of the Ca-B/Na-Alg composite gels are proposed.

EXPERIMENTAL

Materials

Ca-B was obtained from the Enez-Edirne region of Turkey. The raw bentonite samples were dispersed in tap water at room temperature for 48 h and were then subjected to a multistage purification process with a Mozley 750 C 2 inch separator (Mozley group, Gluster, UK.)[20–22] Under optimum conditions, a concentrate product with a cation exchange capacity of 89 mequiv/100 g and an average particle size of 2.5 μm was obtained; this indicated the high purity of the sample. The bentonite sample was initially dried at 60°C, gently ground with a homemade type pestle/mortar machine, and screened to −150 μm for further use. The chemical compositions of the samples were accomplished with an inductively coupled plasma spectrometer from the ACME Analytical Laboratory (Vancouver, BC Canada). Ca-B had the following chemical composition: SiO_2, 54.74 wt %; Al_2O_3, 15.53 wt %; Fe_2O_3, 5.06 wt %; MgO, 3.11 wt %; CaO, 2.51 wt %; Na_2O, 1.7 wt %; and K_2O, 1.51 wt %.

Na-Alg, purchased from Bio-Chemika (Fluka Chemicals, Buchs, Switzerland) as an alginic acid of sodium salt from brown algae, was used in the biocomposite studies. Its grade was specifically recommended for immobilization applications. Analytical-grade $CaCl_2$ (from Panreac, Quimica SA) was used in the experiments.

Methods

A rotational disc viscometer (class programmable Brookfield RVDV-II+ model, Brookfield Engineering Laboratories, Massachusetts) was used for the viscosity measurements. The Ca-B was dispersed in Na-Alg solutions by a laboratory-scale mechanical disperser (maximum = 12,200 rpm) manufactured by Arcelik Co. (Istanbul, Turkey) and formed a gel structure in 5 min. The gel sat overnight and then was used as a stock suspension for further studies. The measured viscosity data were collected and evaluated by Wingather version 1.1 (Brookfield Engineering Laboratories) software.

The electrophoretic mobility of the Ca-B clay particles in the absence and presence of the polymer (0.5–2 wt % Na-Alg) was determined with a microelectrophoresis apparatus (Zeta Meter 3.0+, Zeta-Meter, Inc., Staunton VA, USA). All dispersions were prepared in double-distilled water. The pH of the suspension was measured with a pH meter.

Ca-B/Na-Alg biocomposite films were prepared by casting and solvent evaporation techniques at room temperature. The desired quantity of Na-Alg was hydrated overnight in double-distilled water to facilitate the dissolution of Na-Alg. Desired amounts of Ca-B were added to the Na-Alg solution. This dispersion was directly cast onto a clean glass plate at room temperature. Then, all of the samples were soaked in a 20 wt % $CaCl_2$ solution bath for 0.5 h. The films were washed with double-distilled water to remove the remaining traces of the solvent. The film was then dried at room temperature for 3 days.

The characterization and morphology of the Ca-B added Na-Alg biocomposite systems were investigated with XRD, FTIR spectroscopy, and AFM. XRD measurements of the biocomposite films were performed with a Rigaku Miniflex model X-ray diffractometer equipped with Cu Kα radiation (Rigaku Corporation, Texas, USA) at room temperature. All of the samples were dried in a vacuum oven for overnight at 50°C to remove excess moisture and were then analyzed for moisture content by a Precisa moisture analyzer (model XM60, Dietikon, Switzerland); the nanocomposites showed 6–25% moisture according to the alginate gel content of the nanocomposites. The samples were scanned up to a 2θ of 60° (where θ is the Bragg angle) in a continuous mode. The FTIR spectra for the alginate films and alginate biocomposites after the addition of Ca-B were conducted with a PerkinElmer FTIR spectrometer (Massachusetts, USA).

AFM XE 70, Park System, Korea was used to examine the surface topography of the biocomposite samples. The AFM measurements were carried out with moisture-controlled medium ambient conditions (22 ± 2°C) with noncontact mode. Cantilevers were exposed to UV/O_3 (UV Cleaner, Bioforce Nanosciences, Ames) for 15 min before each experiment to remove contamination on each probe. Section analysis, roughness, and power spectral density measurements were calculated with SPIP nanoscope image analysis software from Image Metrology (Lyngby, Denmark). We prepared each thin slide by cutting the sample perpendicular to the plane. The images were taken on this perpendicular section of the samples during AFM measurements.

RESULTS AND DISCUSSION

The rheological characterization of the Ca-B/Na-Alg biocomposite dispersions composed of 6% solids

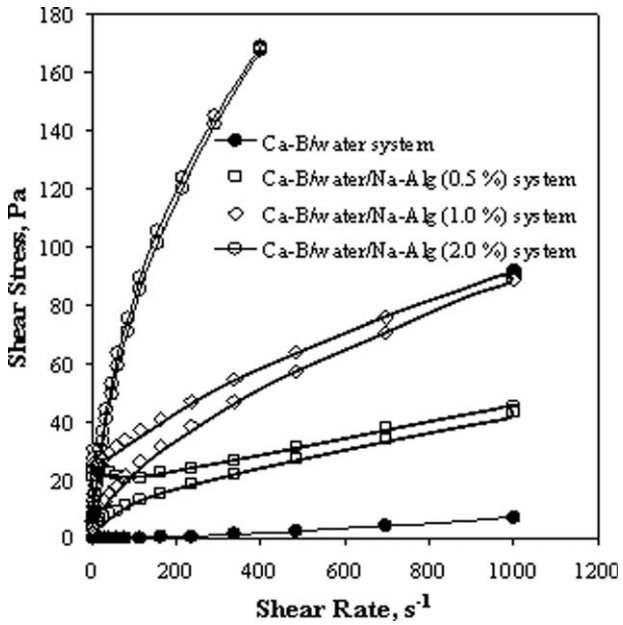

Figure 1 Effect of Na-Alg addition on the rheology of the Ca-B dispersions.

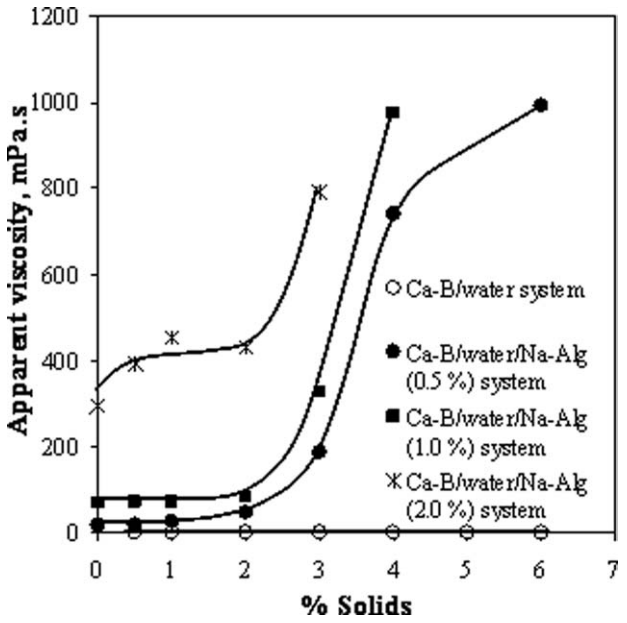

Figure 3 Dependence of the percentage of solids on the apparent viscosity of the Ca-B/Na-Alg biocomposite dispersions.

with 0.5, 1, and 2 wt % Na-Alg is presented in Figure 1. Increasing the concentration of Na-Alg caused an obvious change in the flow curve of the Ca-B/Na-Alg dispersions measured 1 day after the preparation. A similar change was also observed between the apparent viscosity and the shear stress of the dispersions, as given in Figure 2. The apparent viscosity of the dispersions showed a sharp decrease at small shear rates; this indicated the thixotropic nature of the dispersions. Similarly, the apparent viscosity at a low shear rate was higher than that at a high shear rate when a higher content of Na-Alg was incorporated into the gel. It is clear from Figures 1 and 2 that all of the dispersions with and without alginate exhibited non-Newtonian and pseudoplastic flow behaviors. The rheological behavior of the dispersions was best fitted to the Hershel Bulkley model between shear stress, s and velocity gradient, g [$\tau = \tau_c + \kappa\gamma^n$, where τ_c is the yield stress (Pa), κ is the consistency index, and n is the flow index] like other viscoplastic systems such as raw cement,[23] drilling mud,[24] and oil–water emulsions.[25] This rheological model encompasses as limiting cases the Bingham plastic, power law, and Newtonian fluid models. The rheological characteristics of the dispersions, that is, the apparent viscosity, thixotropy, yield stress, and plastic viscosity were determined according to the Hershel Bulkley model and are shown in Figures 3–6, respectively. Increasing the clay concentration in the Ca-B/Na-Alg dispersions clearly caused a pronounced increase, especially after the addition of 3% solids. On the other hand, at concentrations lower than this, the effect of solid loading on the viscosity could be ignored. However, above 2 wt % Ca-B, the effect of the solid concentration was a more predominant factor in the bentonite/alginate system. Above this concentration, similar to that reported by Pongjanyakul and Puttipipatkhachorn,[26] the alginate dispersions flocculated and formed a three-dimensional network structure as gelation. This structure was supported by the easy gelling ability of alginate with the Ca-Alg junction zones; this is popularly known as the *egg-box model*.[4] Furthermore, the area of

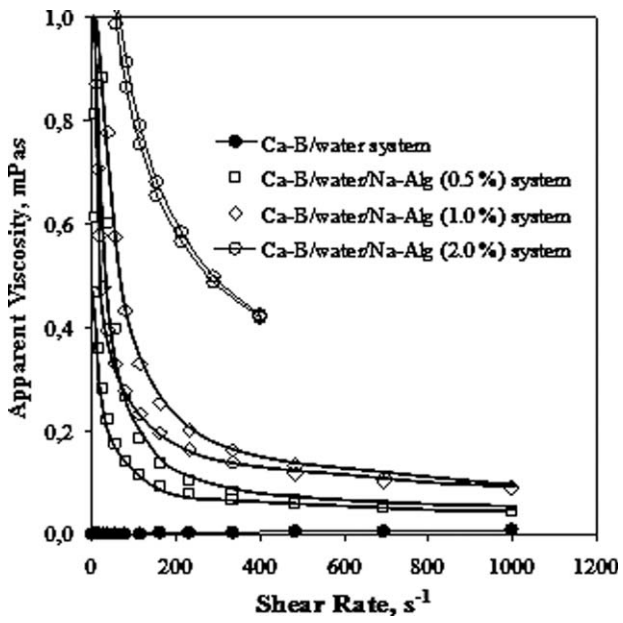

Figure 2 Shear stress–shear rate profiles for various Ca-B/Na-Alg biocomposite dispersions.

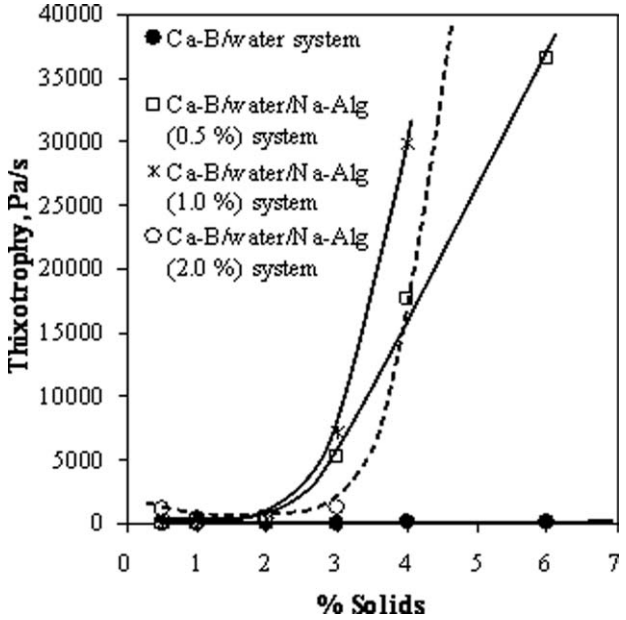

Figure 4 Thixotropy of different Ca-B/Na-Alg biocomposite dispersions as a function of the percentage of solids.

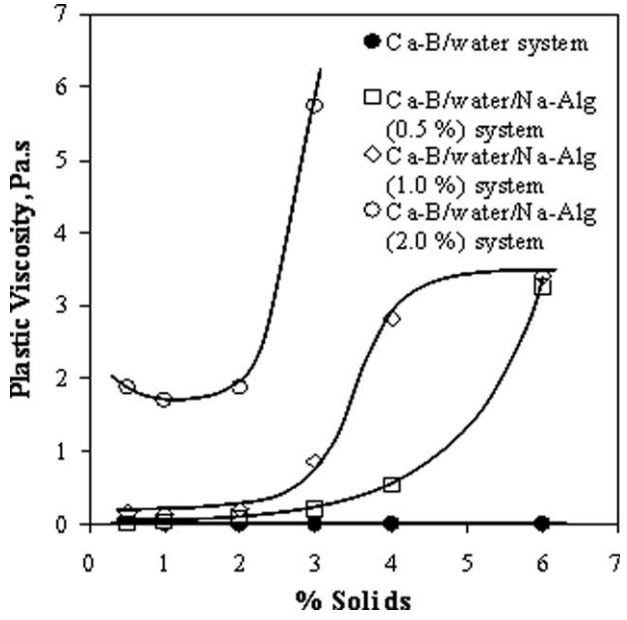

Figure 6 Plastic viscosity of Ca-B/Na-Alg biocomposite dispersions at different percentages of solids.

hysteresis loop between the up curve and the down curve of the flow curve of the composite gels increased with increasing alginate content. This suggested that Ca-B improved the thixotropic properties of the Na-Alg gels, although alginate concentrations above 2% could not be observed because they exhibited a rather high gelation ability[4,27] and made rheological study difficult.[28]

The yield stress data against the percentage clay addition in Figure 5 indicate that interaction between the clay particles and alginate in the dispersion was dependent on the clay concentration; at solids concentrations below 2%, the yield stress values were negligible. At low bentonite additions, the system exhibited features akin to a nanocomposite. However, an increase in the clay concentration led to enhanced interactions and resulted in possible new mechanisms, as ion exchange and encapsulation became more dominant in the Ca-B/Na-Alg system.

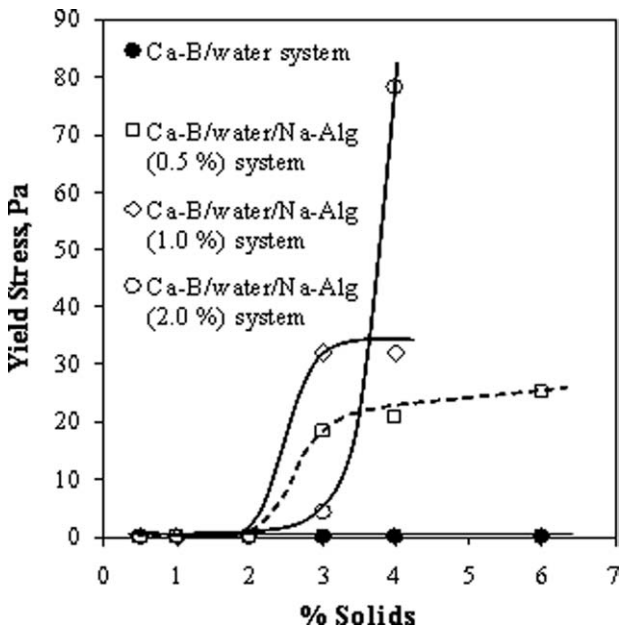

Figure 5 Yield stress of various Ca-B/Na-Alg biocomposite dispersions at different percentages of solids.

Plastic viscosity reflects an increasing yield stress value in suspensions and is indicative of a change in the flow model. As it is known, suspensions generally exhibit pseudo-plastic flow behavior and are represented with the shear stress–shear rate curves starting from the zero point. When the suspension turns into a plastic form (i.e., Bingham plastic), a certain shear stress is required to make the suspension flow, and this point is defined as the *yield stress.* Higher yield stress values show the flow transition from pseudo-plastic to plastic. In this case, the plastic viscosity is required to characterize the suspension. As shown in Figure 6, for Na-Alg concentrations lower than 1%, the plastic viscosities increased with bentonite concentrations higher than 3%. In case of a 2% Na-Alg concentration, a 2% Ca-B addition was found to be the critical concentration for making the suspension more plastic. In addition, dramatic increases in the plastic viscosities also proved that the suspension turned into a rigid gel structure. Figure 6 shows the changes in the plastic viscosities of the suspensions and reveals that both the Na-Alg and Ca-B concentrations played significant roles in keeping the suspension in the gel structure.

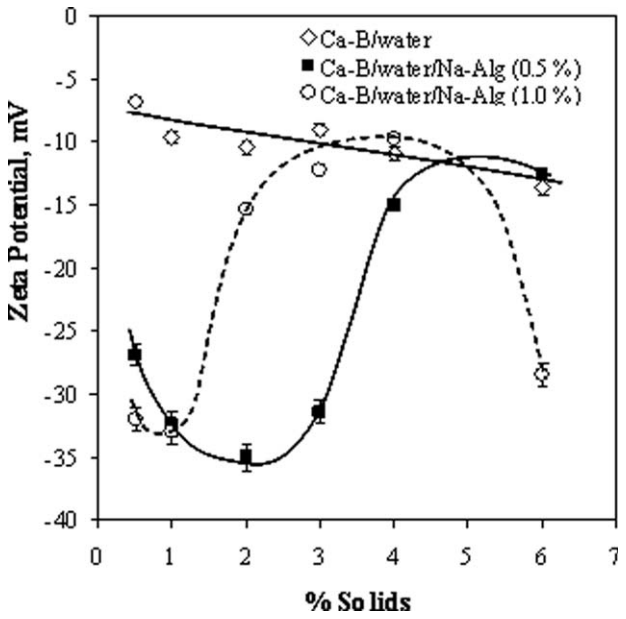

Figure 7 zp versus the percentage of solids for different Ca-B/Na-Alg biocomposite dispersions.

zp is another important indicator in understanding the stability of dispersions. The electrokinetic behavior of the Ca-B added Na-Alg dispersions was measured at natural pH, as shown in Figure 7. The zp values became more positive with increasing alginate concentration from nearly −10 mV (without alginate) to −40 mV for the 2% Na-Alg dispersion. Similar behavior was observed with Unye bentonite of Turkey, with reported zp values of −42.4 mV at a 2 w/w % bentonite addition.[14] These results were in good agreement with the conductivity of the Ca-B added alginate suspensions presented in Figure 8. Ion release to the suspension, which was directly related to the ionic interactions, increased with increasing alginate concentration and reached a peak value at 2% bentonite/2% alginate addition. Both the rheology and the electrokinetic measurements showed that a simple ion-exchange mechanism possibly controlled the behavior of the Ca-B/Na-Alg biocomposite system.

We examined the ionic interactions by measuring the released Na^+ and Ca^{2+} ions to the dispersion to understand the mechanism behind the self-assembly system. Figure 9(a,b) shows the release of Na^+ and Ca^{2+} ions as a function of Ca-B for the 0.5, 1, and 2% Na-Alg dispersions. Ion releases at three different concentrations of Na-Alg were measured at 414, 907, and 1890 ppm for Na^+, and 0.21, 0.21, and 0.42 ppm for Ca^{2+}. As shown in Figure 9, the released ions played a significant role, especially at concentrations below 2%. However, the evidence for incorporating Ca-B into the alginate system could be realized through XRD analyses. Toward this aim, the investigation of the macroscopic parameters of the biocomposite dispersions, that is, the rheology, thixotropy, yield stress, zp, and released ions, were continued on the biocomposite films. XRD patterns of dried $CaCl_2$-crosslinked alginate/bentonite composites were prepared with 1% Na-Alg and different percentage solids of Ca-B, as shown in Figure 10. The calculated basal spacing values of these composites are illustrated in Table I. At solid contents of less than 4% and at 1% Na-Alg, there was no distinct diffraction peak in the range 3–9° (2θ).[29,30] According to Zhou et al.,[16](b) the absence of diffraction peaks could be attributed to two possible reasons: (1) an exfoliated structure and (2) a disordered intercalated structure with an average *d*-spacing higher than 7 nm. In this region, similar to the zp and ion-release measurements, the diffraction peaks were interpreted as higher level interactions between Ca-B and Na-Alg. On the other hand, the preparation of denser composites (0.5 wt % Na-Alg with 1 and 4% Solids Ca-B) were also found to decrease the diffraction peaks (Fig. 11); this was in line with the results of Darder et al.[31] for chitosan, a natural biopolymer. At solid contents of both 4 and 1%, the significant diffraction peaks shifted to 2θ's of about 5.83 and 4.99, respectively, from that of bare Ca-B due to the intercalated and flocculated structures.[17] Possible structural models of the Ca-B/Na-Alg composite gels are illustrated in Figure 12. There were three different mechanisms, depending on the solid content variation

1. At low solid contents, bentonite in the alginate solution was distributed as exfoliated or disordered.

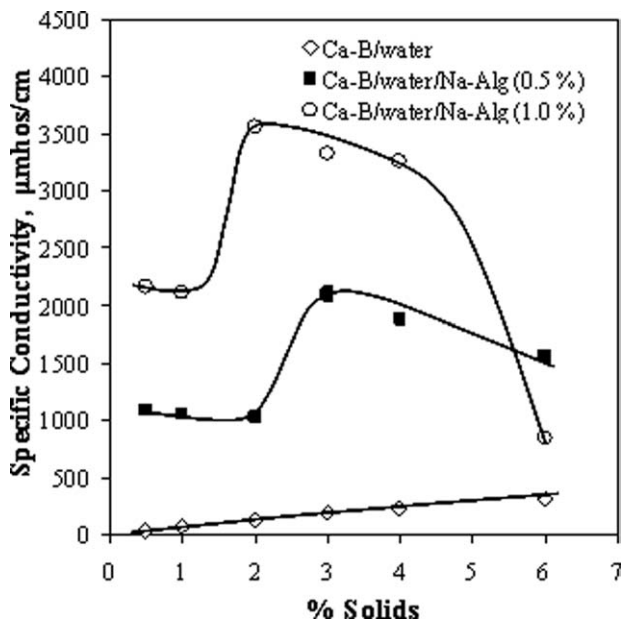

Figure 8 Variation of the specific conductivity with the percentage of solids for different Ca-B/Na-Alg biocomposite dispersions.

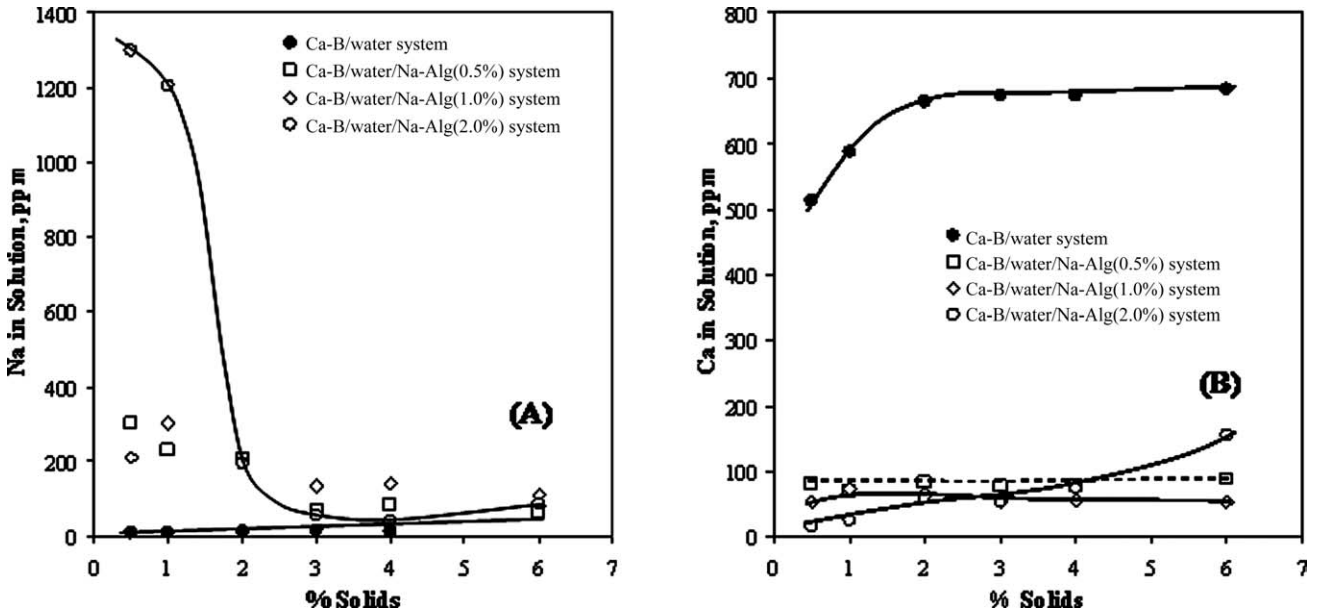

Figure 9 Ion release from the Ca-B/Na-Alg biocomposite dispersions versus the percentage of solids for (A) sodium and (B) calcium.

2. At moderate solid contents, bentonite was intercalated.
3. At high Ca-B addition, the magnitude of exchanged ions increased in the solution, and then, exchangeable ions, mostly divalent Ca^{2+}, Mg^{2+}, and Al^{3+}, were exchanged and crosslinked with Na-Alg followed by encapsulation.

Depending on the slow gelatinization process between Ca-B and Na-Alg, crystallinity and a more perfect ordering of the Ca-Alg gel beads were formed with large pieces, as shown in Figure 12. Slow gelling processes are expected to provide better structural information about the junction zones alginate gels.[27] This result is very important for biocomposite, drug delivery, tissue engineering, biomedical, and encapsulation studies because of the difficulty in designing selective ionic interactions with Ca^{+2} ions between the Ca-B and Na-Alg solutions as activator, modifier, and/or gelling agent. The conditioning of Na-Alg with the Ca-B activated the bentonite structure to the Na form of bentonite with an ion-exchangeable mechanism. On the other hand, at higher Ca-B concentrations, more divalent cations, in our case, Ca^{+2} ions, were released from Ca-B, and thus, encapsulation may have been a more dominant mechanism for the Ca-B/Na-Alg system. This system may be regarded as an excellent example of a self-assembling process, which refers to the assembly of building blocks of various natures, from organic molecules and polymers to inorganic entities.[32] After the partial protonation of carboxylate groups in the alginate molecules, these partially crosslinked alginate assemblies are pH-sensitive.[33]

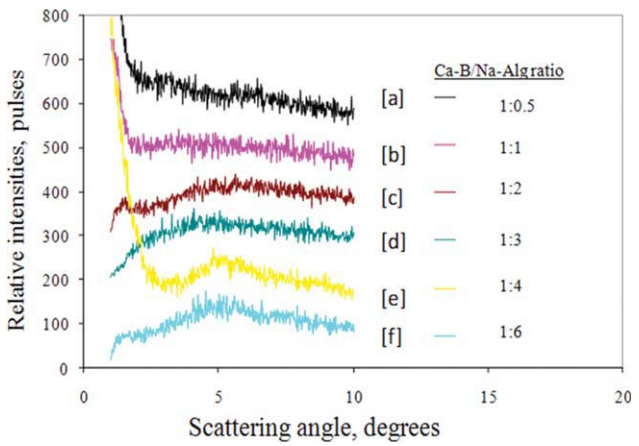

Figure 10 XRD data of the Ca-B/Na-Alg biocomposite solution (1 wt %) with solid concentrations of Ca-B of (a) 0.5, (b) 1, (c) 2, (d) 3, (e) 4, and (f) 6%. [Color figure can be viewed in the online issue, which is available at wileyonlinelibrary.com.]

AFM images of the composite samples further helped to identify the morphologies of the bentonite dispersion, as illustrated in Figure 13(a–c).

TABLE I
2θ Values Obtained for the Ca-B/Na-Alg Biocomposites

Bentonite concentration in a 1% Na-Alg solution	2θ	*d*-spacing (Å)
0.5	No peak	
1	1.21	73.11
2	1.59	55.65
2	4.08	21.68
3	1.81	48.78
4	4.99	17.70
6	5.83	15.15

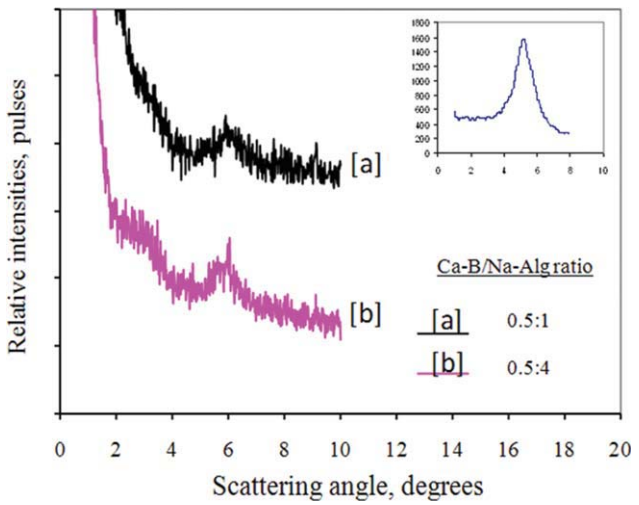

Figure 11 XRD data of the Ca-B/Na-Alg biocomposite solution (0.5 wt %). [Color figure can be viewed in the online issue, which is available at wileyonlinelibrary.com.]

Individual bentonite particles were found on the nanocomposite surface with a Phase AFM image in noncontact mode at 5 μm^2/scanning area. As encapsulated bentonite was observed in Figure 13(c), the ion-exchange mechanism was directly confirmed in the higher Ca-B added Na-Alg structures. According to Cao et al.,[33] at neutral pH values, because of the ionization of carboxylic acid groups, the hydrogen bonds between carboxylic groups will be destroyed, and the structures will be disintegrated. Therefore, in our case, the increasing bentonite ratio in the aqueous system was one of the main reasons for the increase in the pH of the system. At this relatively high pH, the disintegration of the composite structure and the encapsulation of disordered bentonite between the crosslinked alginate molecules was expected. This proposed structure is presented in Figure 13(c).

In addition, the possible structures of composite systems for 1% Na-Alg at different Ca-B solid concentrations were confirmed by FTIR spectroscopic analyses, shown in Figure 14. The assignments of the functional groups available in the Ca-B/Na-Alg biocomposite against the absorption band assignments[34,35] are listed in Table II. The characteristic band of alginate was observed at 3353 cm^{-1} for the hydroxyl groups and at 1611 and 1431 cm^{-1} for the asymmetric —COOH stretching vibrations and

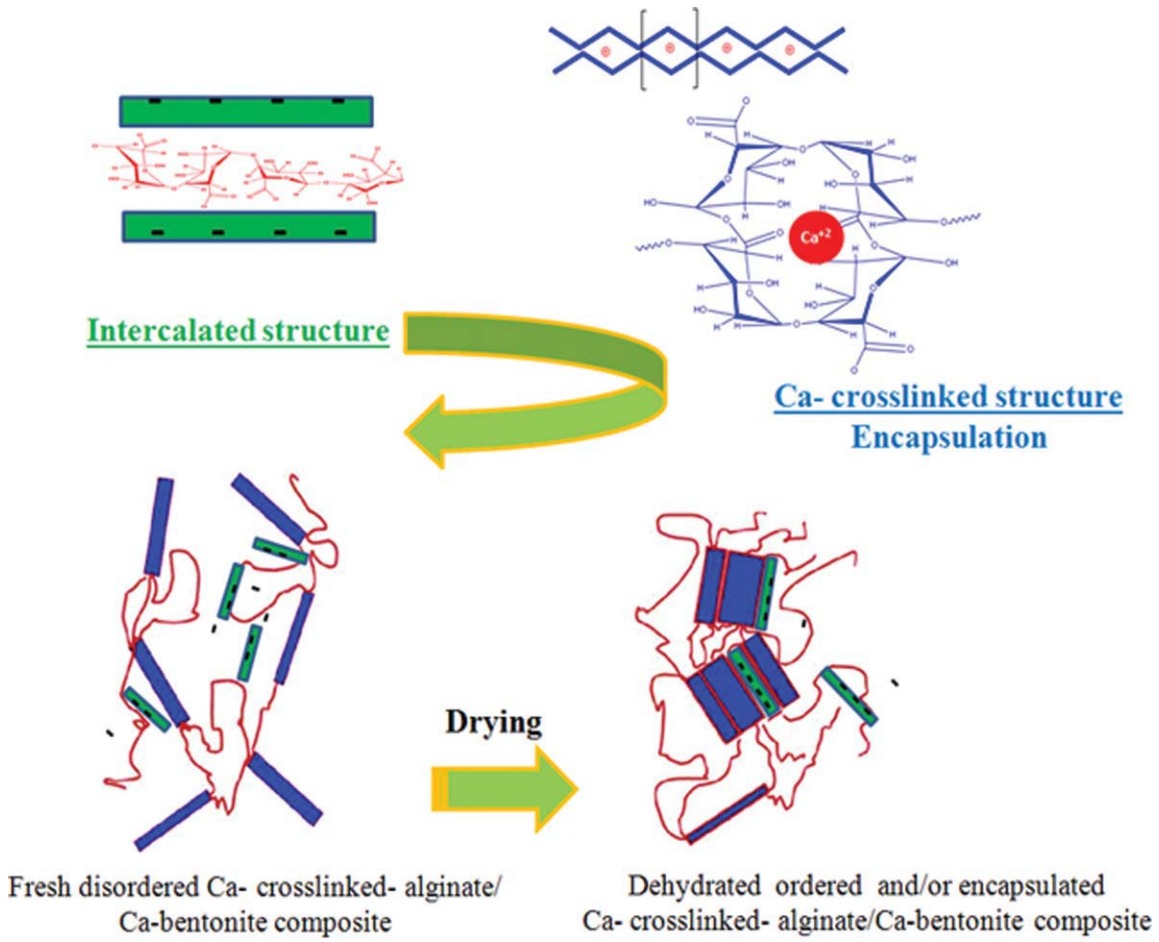

Figure 12 Possible interaction mechanisms between the Ca-B and Na-Alg biocomposite systems. [Color figure can be viewed in the online issue, which is available at wileyonlinelibrary.com.]

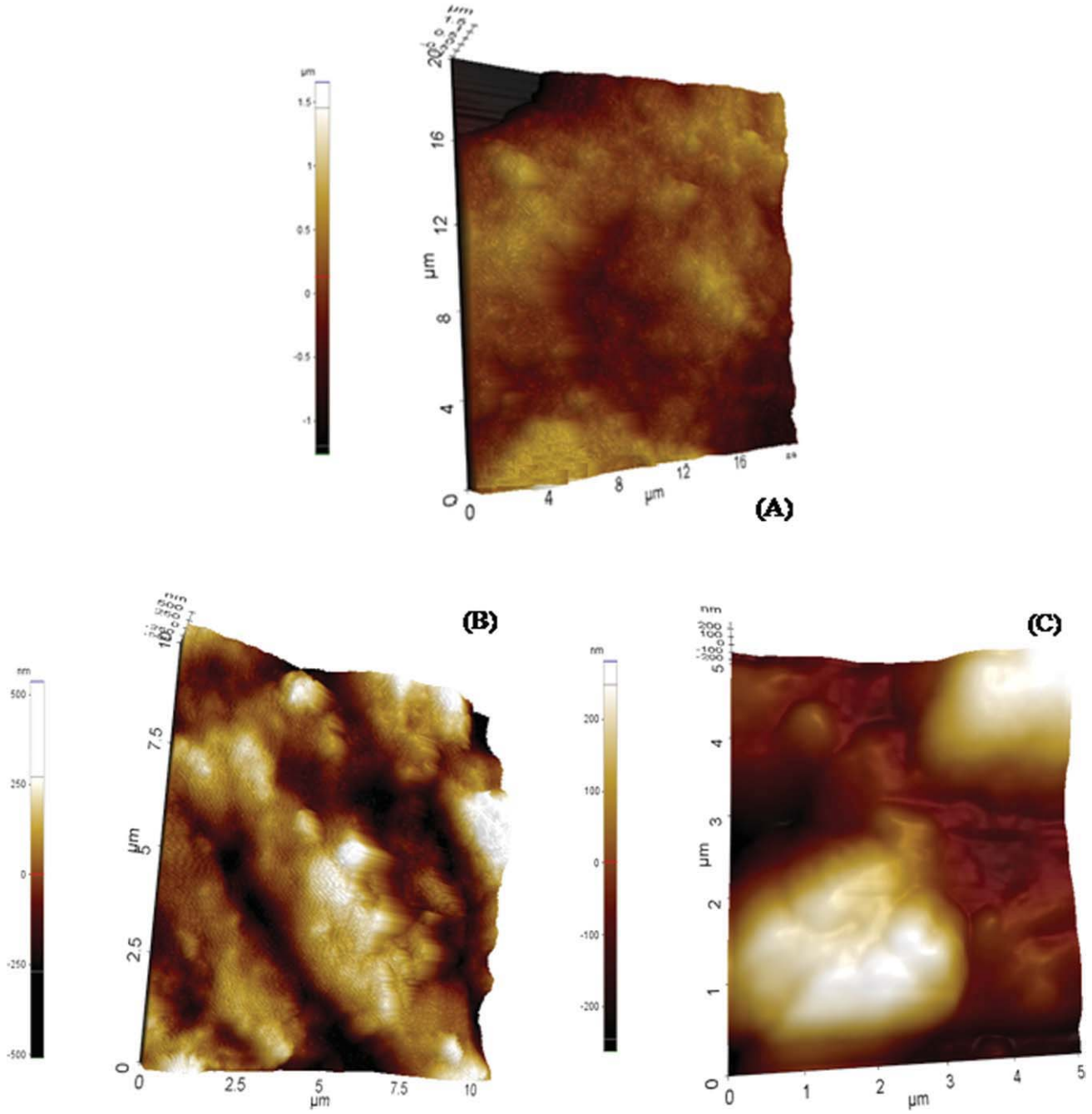

Figure 13 AFM images of the Ca-B/Na-Alg biocomposites with (A) a 0.5% solid ratio of Ca-B in 1 wt % alginate, (B) a 1% solid ratio of Ca-B in 1 wt % alginate, and (C) a 6% solid ratio of Ca-B in 1 wt % alginate. [Color figure can be viewed in the online issue, which is available at wileyonlinelibrary.com.]

symmetric —COOH stretching vibrations. On the other hand, the characteristic bands of clay at 3622, 1033, 914, and 790 cm^{-1} for the Al—O—H stretching, Si—O—i, Si—O stretching, Al—O—H, Si—O stretching, Si—O—Al stretching, and (Al, Mg)— O—H and Si—O—(Mg, Al) stretching were not observed at small bentonite additions because of the composite structure. Above a 4% solid content of bentonite, these peaks started to become noticeable.

The OH stretching peak between 3360 and 3352 cm^{-1} became a little bit narrower at 1 wt % Ca-B addition and, then, remained similar at higher Ca-B ratios with a lesser intensity. The C—H peak at 2981 cm^{-1} was also seen at a 6% solid content of Ca-B. Because the conditioning time of Ca^{2+} ions is very critical to the composite structure and ion-exchange mechanism of the system;[34] this was evidence for the characteristic increase in intramolecular bonding at smaller ratios and, conversely, a decrease in the intramolecular bonding at higher solid ratios. The rheology, ion release, zp, and AFM images also confirmed this finding.

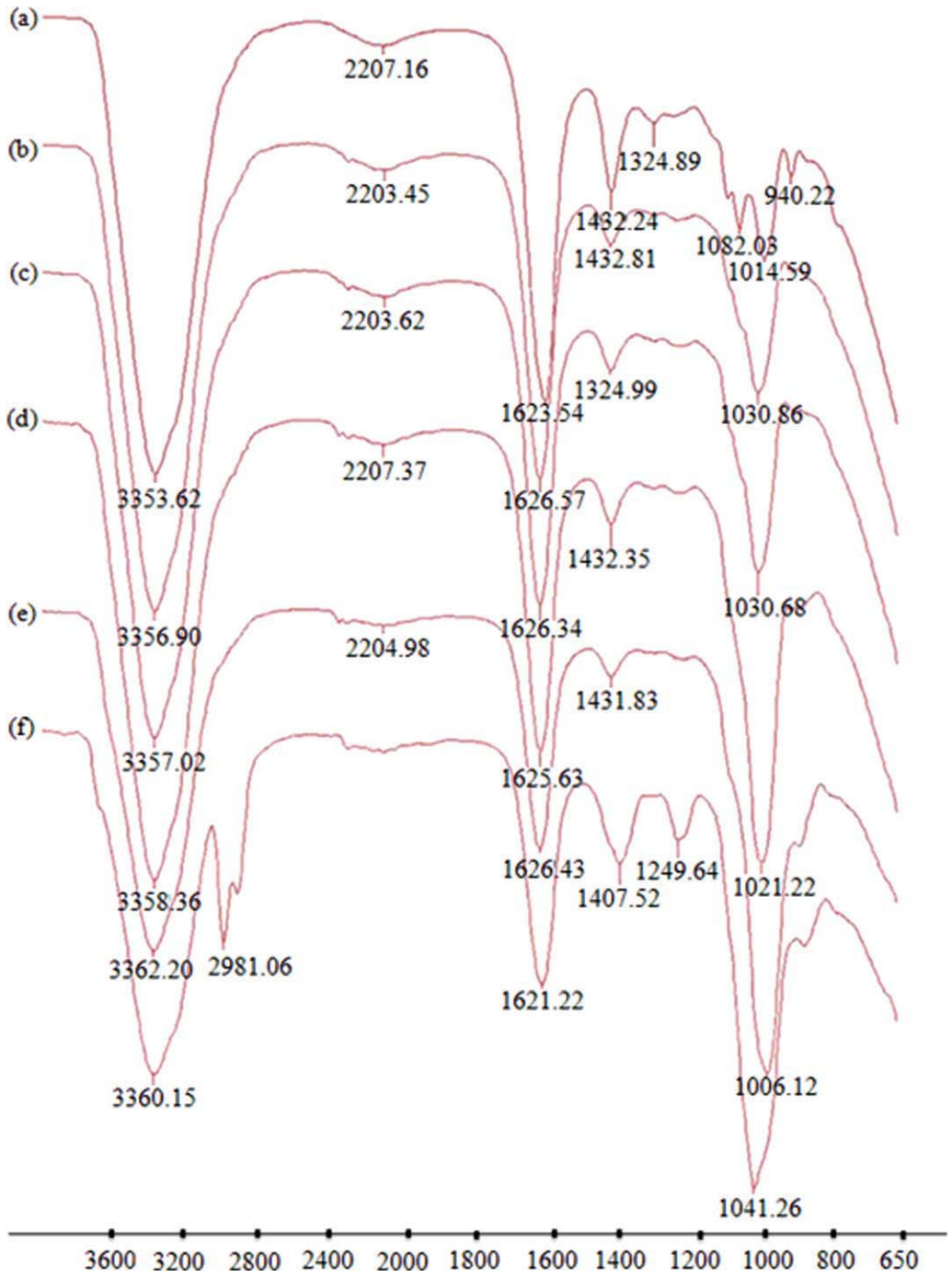

Figure 14 FTIR spectra of the Ca-B/Na-Alg biocomposites with 1 wt % alginate with different solid concentrations of Ca-B: (a) 0.5, (b) 1, (c) 2, (d) 3, (e) 4, and (f) 6% (from top to bottom). [Color figure can be viewed in the online issue, which is available at wileyonlinelibrary.com.]

The spectra of the Ca-B/Na-Alg biocomposite films were characterized by the presence of absorption bands typical of the pure components, with the intensity roughly proportional to the mixing ratio. The peak at 1611 cm^{-1} shifted to 1625 and 1626 cm^{-1}; this suggested the presence of new hydrogen bonds between alginate and bentonite. This was ascribed to the electrostatic interaction between such groups and the negative sites on the clay structure.[30] Furthermore, the peak at 1431 cm^{-1}, which represented the stretching vibration of carboxylate groups, shifted to a lower frequency (1407 cm^{-1}) in the corresponding nanocomposite spectra.[36] This peak was also specific to ionic binding resulting from the calcium ions' replacement with sodium ions in the alginate blocks.[34] However, at higher bentonite additions, the Si—O stretching peak shifted and exhibited a maximum at 1041 cm^{-1}; the

TABLE II
Assignments of the FTIR Absorption Bands for the Ca-B/Na-Alg Biocomposites

Wave number (cm^{-1})	Assignment
3622	Al—O—H stretching
3360–3380	O—H stretching
2750	C—H stretching
1608–1611	COO— stretching (asymmetric)
1413–1414	COO— stretching (asymmetric)
1124–1126	C—C stretching
	C—O stretching
1087–1088	C—O stretching
	C—O—C stretching
1059	O—H bending
1033	Si—O—Si, Si—O stretching
947–950	C—O stretching
	C—H stretching
914	Al—O—H stretching
790	Si—O stretchingSi—O—Al stretching
	(Al, Mg)—O—H stretching
	Si—O—(Mg, Al) stretching

structural Al—O vibration at 914 cm^{-1} also confirmed the presence of bentonite in the dispersions.[14] The peaks in the range 1150–1000 cm^{-1} were assigned to C—C and C—O bonds, most likely because these bonds were shared with the calcium ions, namely, Ca crosslinking of alginate as evidence of the encapsulation of bentonite.

CONCLUSIONS

The flow behavior and electrokinetic properties of Ca-B/Na-Alg biocomposite systems showed that the extent of exchangeable cations of bentonite was very important in the formation of the alginate biocomposite systems. In the presence of Ca ions, because of the electrostatic forces and intermolecular hydrogen bonding between Ca-B and Na-Alg, a denser matrix structure was formed with increasing junction zones of the composite gels by the partially crosslinked alginate; this is popularly known as the *egg-box model*. The incorporation of Ca-B into the Na-Alg gels or vice versa provided a higher viscosity and changed the flow behavior from Newtonian to pseudo-plastic with thixotropy. During this process, Ca-B was activated by Na ions released from the Na-Alg. It was confirmed that the conditioning time of the Ca^{2+} ions in the alginate dispersions was very critical to the structure of composite formation and ion-exchange mechanism of the system. The variations in pH and the content of Ca^{2+} ions provided an excellent example of a self-assembling process.

References

1. Lu, J. W.; Zhu, Y. L.; Guo, Z. X.; Yu, J. Polymer 2006, 47, 8026.
2. Roger, S.; Talbot, D.; Bee, A. J Magn Magn Mat 2006, 305, 221.
3. Benli, B.; Nalaskowski, J.; Assemi, S.; Celik, M. S.; Miller, J. D. J Adhes Sci Technol, to appear.
4. Grant, G. T.; Morris, E. R.; Rees, D. A.; Smith, P. J. C.; Thom, D. FEBS Lett 1973, 32, 195.
5. Ma, P. X.; Elisseeff, J. H. In Scaffolding in Tissue Engineering; CRC, Taylor & Francis: Washington, DC, 2006; p 304.
6. Miraftaba, M.; Qiaoa, Q.; Kennedy, J. K.; Ananda, S. C.; Groocock, M. R. Carbohydr Polym 2003, 53, 225.
7. Moon, S. C.; Ryu, B. Y.; Choi, J. K.; Jo, B. W.; Farris, R. J. Polym Eng Sci 2009, 49, 52.
8. Martins, S.; Sarmento, B.; Souto, E. B.; Domingos, C. F. Carbohydr Polym 2007, 69, 725.
9. Gbassi, G. K.; Vandamme, T.; Ennahar, S.; Marchioni, E. Int J Food Microbiol 2009, 129, 103.
10. Pranoto, Y.; Salokhe, V. M.; Rakshit, S. K. Food Res Int 2005, 38, 267.
11. Haugaard, V. K.; Udsen, A. M.; Mortensen, G.; Høegh, L.; Petersen, K.; Monahan, F. Starch 2001, 53, 189.
12. Wong, M. In Biopolymer Methods in Tissue Engineering; Hollander, A. P., Hatton, P. V., Eds.; Methods in Molecular Biology; Humana: Totowa, NJ, 2003; pp 77, 238.
13. Tan, K. H. Principles of Soil Chemistry, 3rd ed.; MarcelDekker: New York, 1998; p 190.
14. Günister, E.; Pestreli, D.; Ünlü, C. H.; Atıcı, O. Carbohydr Polym 2007, 67, 358.
15. Isci, S.; Günister, E.; Ece, I.; Güngör, N. Mater Lett 2004, 58, 1975.
16. (a) Yang, L.; Liang, G.; Z, Z.; He, S.; Wang, J. J Appl Polym Sci 2009, 114, 1235; (b) Zhu, J.; Wang, X.; Tao, F.; Xue, G.; Chen, T.; Sun, P.; Jin, Q.; Ding, D. Polymer 2007, 48, 7590.
17. Ray, S. S.; Okamoto, M. Prog Polym Sci 2003, 28, 1539.
18. Armagan, B.; Ozdemir, O.; Turan, M.; Celik, M. S. J Chem Technol Biotechnol 2003, 78, 725.
19. Yang, Y.; Han, S.; Fan, Q.; Ugbolue, S. C. Text Res J 2005, 75, 622.
20. Boylu, F.; Çinku, K.; Esenli, F.; Çelik, M. S. Int J Miner Proc 2010, 94, 196.
21. Bain, J. A.; Morgan, D. J. Clay Miner 1982, 18, 33.
22. Bloodworth, A. J.; Morgan, D. J.; Briggs, D. A. Clay Miner 1989, 24, 539.
23. Lachemet, A.; Touil, D.; Belaadi, S.; Bentaieb, N.; Frances, C. J Appl Sci 2008, 8, 3485.
24. Coussot, P.; Piau, J. M. Rheol Acta 1994, 33, 175.
25. Derkatch, S. R.; Voronko, N. G.; Izmailova, V. N. Int J Appl Mech Eng 2001, 6, 659.
26. Pongjanyakul, T.; Puttipipatkhachorn, S. AAPS PharmSciTech 2007, 8(3), E1.
27. Li, L.; Fang, Y.; Vreeker, R.; Appelqvist, I. Biomacromolecules 2007, 8, 464.
28. Voronko, N. G.; Derkach, S. R.; Izmailova, V. N. Macromol Chem Polym Mater 2002, 75, 808.
29. Park, J. H.; Karim, M. R.; Kim, I. K.; Cheong, I. W.; Kim, J. W.; Bae, D. G.; Cho, J. W.; Yeum, J. H. Colloid Polym Sci 2010, 288, 115.
30. Darder, M.; Colilla, M.; Ruiz-Hitzky, E. Chem Mater 2003, 15, 3774.
31. Darder, M.; Colilla, M.; Ruiz-Hitzky, E. Appl Clay Sci 2005, 28, 199.
32. Parhi, P.; Ramanan, A.; Ray, A. R. J Appl Polym Sci 2006, 102, 5162.
33. Cao, Y.; Shen, X.; Chen, Y.; Guo, J.; Chen, Q.; Jiang, X Biomacromolecules 2005, 6, 2189.
34. Sartori, C.; Finch, S. D.; Ralph, B. Polymer 1997, 38, 43.
35. Nayak, P. S.; Singh, B. K. Bull Mater Sci 2007, 30, 235.
36. Darder, M.; Lopez-Blanco, M.; Aranda, P.; Leroux, F.; Ruiz-Hitzky, E. Chem Mater 2005, 17, 1969.